Optimising NMR Spectroscopy through Method and Software Development

Jonathan Yong

University of Oxford

Contents

refsection:1

refsection:2

refsection:3

refsection:4

Chapter 4

NOAH

chpt:noah

This final—and long—chapter describes my work on *NOAH* (NMR by Ordered Acquisition using ^{1}H detection) *supersequences*, pulse sequences which record multiple 2D datasets (‘*modules*’) in the time required for one. This is an attractive NMR technique for several reasons: the time savings are clearly a key factor, but the flexibility of being able to combine almost any set of modules also makes NOAH supersequences applicable to a variety of contexts.

I begin by introducing the concepts underlying NOAH supersequences, as well as a general discussion of the time savings (and sensitivity per unit time) benefits thus realised. I then describe the GENESIS (GENEration of Supersequences In Silico) website, which allows users to generate Bruker pulse programmes for almost every imaginable NOAH supersequence. After this, my work on various aspects of the actual sequences themselves is described, with a special focus on newly developed and/or improved modules. Finally, the design of ‘parallel’ supersequences which use interleaved and/or time-shared modules is discussed.

This work was done in close collaboration with Ēriks Kupče (Bruker UK). However, all results and analysis shown in this chapter are mine. The work in this chapter forms the subject of several publications:

- Yong, J. R. J.; Hansen, A. L.; Kupče, Ē.; Claridge, T. D. W. Increasing sensitivity and versatility in NMR supersequences with new HSQC-based modules. *J. Magn. Reson.* **2021**, *329*, 107027, DOI: 10.1016/j.jmr.2021.107027
- Kupče, Ē.; Yong, J. R. J.; Widmalm, G.; Claridge, T. D. W. Parallel NMR Supersequences: Ten Spectra in a Single Measurement. *JACS Au* **2021**, *1*, 1892–1897, DOI: 10.1021/jacsau.1c00423
- Yong, J. R. J.; Kupče, Ē.; Claridge, T. D. W. Modular Pulse Program Generation for NMR Supersequences. *Anal. Chem.* **2022**, *94*, 2271–2278, DOI: 10.1021/acs.analchem.1c04

964

- Yong, J. R. J.; Kupče, Ē.; Claridge, T. D. W. Uniting Low- and High-Sensitivity Experiments through Generalised NMR Supersequences. **2022**, manuscript in preparation

The material in the introductory sections also closely follow two reviews which I have contributed to:

- Kupče, Ē.; Frydman, L.; Webb, A. G.; Yong, J. R. J.; Claridge, T. D. W. Parallel nuclear magnetic resonance spectroscopy. *Nat. Rev. Methods Primers* **2021**, *1*, No. 27, DOI: 10.1038/s43586-021-00024-3
- Yong, J. R. J.; Kupče, Ē.; Claridge, T. D. W. In *Fast 2D solution-state NMR: concepts and applications*, Giraudeau, P., Dumez, J.-N., Eds., forthcoming, 2022

4.1 Introduction

sec:noah__introduction

The characterisation of small molecules and biomolecules by NMR spectroscopy relies on a suite of standard 2D NMR experiments, which seek to detect heteronuclear scalar couplings (e.g. HSQC and HMBC), homonuclear scalar couplings (e.g. COSY and TOCSY), or through-space interactions (e.g. NOESY and ROESY). Although 2D experiments provide far superior resolution and information content compared to 1D spectra, they also require substantially longer experiment durations, as the indirect dimension must be constructed through the acquisition of many t_1 increments. This problem is further exacerbated by the fact that structural elucidation or verification often necessitates the acquisition of several different 2D experiments.

The acceleration of 2D NMR has thus proven to be a popular area of research. We may broadly categorise existing techniques into two classes: firstly, those which seek to directly speed up the acquisition of *individual* 2D spectra, and secondly, *multiple-FID* experiments which aim to collect two or more 2D spectra in the time required for one.* The former category includes methods such as non-uniform sampling (NUS),[7–10] fast pulsing (i.e. shortening of recovery delays),[11–14] ultrafast NMR,[5,15–19] Hadamard encoding,[20,21] and spectral aliasing;[22–24] whereas the latter encompasses time-shared NMR,[25,26] multiple-receiver NMR,[27–29] and—of course—NOAH supersequences.[5,30,31]

The scope of this introductory section will be limited to only NOAH supersequences. However, many of these techniques are closely related, and I will introduce concepts from elsewhere as needed. It should be noted that there are several other multiple-FID experiments which, while not explicitly advertised as such, are conceptually identical to NOAH experiments.[32–35] I do not discuss these here.

4.1.1 Time savings and sensitivity analyses

subsec:noah__snr

In a typical 2D NMR experiment, the majority of the experiment duration is taken up by the *recovery delay*—the time required for spins to return to their equilibrium polarisation, such that the next transient or t_1 increment can be recorded. The removal (or shortening) of recovery delays is thus a very effective way of speeding up 2D data acquisition. In NOAH supersequences, 2D experiments ('modules') can be directly concatenated without the addition of extra recovery delays between them: only one overall recovery delay is required for the entire supersequence. This means that, to a first approximation, a supersequence containing N modules ($N \geq 2$) can be acquired in the time needed for just one module. Figure 4.1 shows an example of a NOAH supersequence formed from two modules (HSQC and COSY): the various timings referred to in

*These are by no means mutually exclusive: many of the techniques here can be combined to provide even greater efficiency.

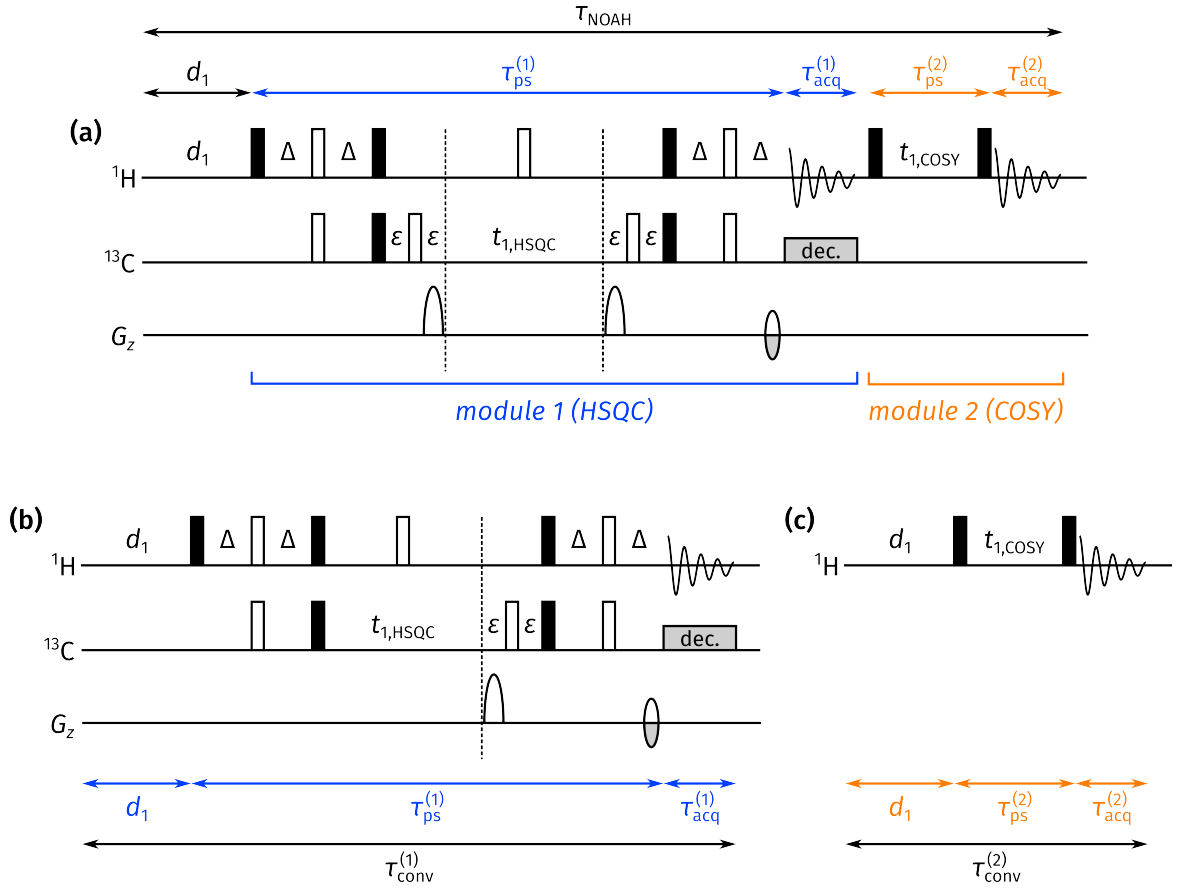

Figure 4.1: **(a)** NOAH-2 SC supersequence, comprising HSQC and COSY modules (see table 4.1 for an explanation of the single-letter module codes used). **(b)** 'Conventional' echo–antiecho HSQC (the same as in fig. 1.7). **(c)** 'Conventional' COSY. The timings referred to in the text are highlighted for all three experiments; I have assumed that d_1 for each experiment is the same. Note that the lengths are not to scale: d_1 is typically far longer than the τ_{ps} and τ_{acq}.

the text which follows are also marked on the diagram.

The duration of an NMR experiment, τ_{exp}, can be expressed as a sum of its parts:

$$\tau_{exp} = \tau_{ps} + \tau_{acq} + d_1, \tag{4.1}$$ {eq:exp_duration_2d}

where τ_{ps} is the time required for the pulse sequence itself (typically several milliseconds), τ_{acq} is the acquisition time (several hundred milliseconds), and d_1 is the recovery delay (one or more seconds). The *time-saving factor* ρ_t for a NOAH supersequence, as compared to a series of conventional standalone experiments, is then:

$$\rho_t = \frac{\sum_i \tau_{conv}^{(i)}}{\tau_{NOAH}} = \frac{\sum_i (\tau_{ps}^{(i)} + \tau_{acq}^{(i)} + d_1^{(i)})}{d_1 + \sum_i (\tau_{ps}^{(i)} + \tau_{acq}^{(i)})}, \tag{4.2}$$ {eq:rho_t}

where τ_{NOAH} is the duration of the NOAH experiment, τ_{conv} is the duration of a conventional

experiment, and the superscript (i) represents the i-th module or conventional experiment being acquired. The sum runs from $i = 1$ to N, where N is the number of modules. If we assume that $d_1^{(i)} = d_1$ is the same for all N conventional experiments and the supersequence, then in the limit where

$$d_1 \gg \sum_i \tau_{\text{ps}}^{(i)} + \tau_{\text{acq}}^{(i)}, \tag{4.3}$$ {eq:d1_limit}

we have that $\rho_t \to N d_1/d_1 = N$. This analysis makes plenty of assumptions, and is not entirely valid in practice. For example, *each* τ_{acq} is often around 5–10% of d_1, so is not entirely negligible, especially in longer supersequences. Furthermore, some modules require longer τ_{ps}: most notable is the NOESY module, which contains a mixing time of several hundred milliseconds. (HMBC, TOCSY, and ROESY spectra are also lesser offenders.) These factors serve to reduce ρ_t from its idealised value of N; generally, this deviation is larger as N increases, because eq. (4.3) becomes less and less valid. Nevertheless, the general point that time savings are approximately proportional to N stands.

For relatively concentrated samples, where sensitivity is not an issue, we can in fact end the discussion here. In this *sampling-limited regime*, the minimum 2D experiment duration is dictated purely by the number of t_1 increments needed to obtain sufficient resolution in the indirect dimension, as well as the minimum phase cycle required for artefact suppression.* NOAH supersequences are identical to conventional experiments in both aspects, but provide a time-saving factor of $\rho_t \sim N$.

The development of modern NMR instrumentation, including high-field magnets and cryogenic probes, means that the sampling-limited regime continues to be extended to ever lower concentrations. However, it is often not this simple: the opposite *sensitivity-limited regime* is still very commonly encountered, for example with naturally insensitive experiments (e.g. ADEQUATE), low-field benchtop NMR, or most simply, dilute samples.†

In such cases, it becomes mandatory to compare the SNRs of the NOAH modules and conventional experiments. To do so, we define for each module an *SNR factor* $A^{(i)}$, which is the SNR of the NOAH module divided by the SNR of a conventional experiment, acquired with the same parameters.‡ In general, we have that $A \leq 1$, because NOAH modules frequently contain small modifications from conventional experiments (as will be explained in § 4.1.2). The *gain in*

*With modern gradient-enhanced experiments, the minimum phase cycle may well not even be a 'cycle'; see also fig. 1.8.

†If the SNR factor $A^{(i)}$ as discussed below is *very small*, then it is possible that even concentrated samples may be shifted into the sensitivity-limited regime. This is never really the case in practice, though, as will be shown in § 4.1.3.

‡The relative SNR will likely vary from peak to peak in the spectrum, and $A^{(i)}$ should in theory be quoted either as an average over all peaks, or as a range. This is what I have done in this thesis. However, comparisons in the literature are not always as thorough.

sensitivity per unit time, $\varepsilon^{(i)}$, is then defined by

$$\varepsilon^{(i)} = A^{(i)}\sqrt{\rho_t}, \tag{4.4}$$ {eq:varepsilon_i}

where the square root accounts for the fact that SNR scales only as the square root of the number of scans, or the number of times the experiment can be repeated in a given period. Of course, the exact values calculated for $A^{(i)}$ (and hence $\varepsilon^{(i)}$) will depend on the sample chosen for the comparison. These values should therefore be assumed to be valid only for similar samples.

If $\varepsilon^{(i)} > 1$, as is frequently the case, this means that the NOAH supersequence provides greater sensitivity per unit time in the i-th module compared to a standalone experiment. Equivalently, performing a NOAH experiment allows data of sufficient sensitivity to be obtained in less time. Naturally, this condition is most important for modules which are inherently insensitive, particularly heteronuclear correlation modules. For sensitive (typically homonuclear) modules, it is often perfectly tolerable to have $A < 1$ or even $\varepsilon < 1$, as even with this sensitivity penalty they are still more intense than the heteronuclear modules.

Another issue with NOAH supersequences is that each module is run with the same number of scans (phase cycle). Although this was touted as a benefit in the sampling-limited regime, this may in fact be undesirable in the sensitivity-limited regime, where insensitive experiments need to be run with more scans than sensitive ones. In this case, the *effective* time savings provided by NOAH experiments are smaller:

$$\rho_{t,\mathrm{eff}} = \frac{\sum_i \tau_{\mathrm{conv}}^{(i)}}{\tau_{\mathrm{NOAH}}} = \frac{\sum_i S^{(i)}(\tau_{\mathrm{ps}}^{(i)} + \tau_{\mathrm{acq}}^{(i)} + d_1^{(i)})}{Sd_1 + S\sum_i(\tau_{\mathrm{ps}}^{(i)} + \tau_{\mathrm{acq}}^{(i)})}, \tag{4.5}$$ {eq:rho_t_eff}

where each standalone experiment is acquired with $S^{(i)}$ scans and the NOAH experiment with S scans. Typically, S is simply the largest of the $S^{(i)}$. If $S^{(i)} = S$ for all i, then eq. (4.5) simply reduces to eq. (4.2); on the other hand, if the $S^{(i)}$'s are different, then we have that $\rho_{t,\mathrm{eff}} < \rho_t$. In such a situation, it is probably more appropriate to describe a NOAH supersequence as 'measuring the most insensitive module and getting the others for free'. Indeed, if $S = S^{(i)} \gg S^{(j\neq i)}$, then 'the other' modules require almost no time to measure (relative to the least sensitive module), and $\rho_{t,\mathrm{eff}}$ tends towards 1, meaning that even the time-saving utility of NOAH vanishes. A corollary of this is that NOAH supersequences are generally best constructed from modules which have similar intrinsic sensitivities and hence similar $S^{(i)}$'s.

As the reader can no doubt appreciate by now, the comparison of NOAH and conventional spectra is fraught with subtleties (which are sometimes glossed over in the literature, but invariably surface in real-life discussions). In fact, it is hardly even difficult to construct yet more edge cases. For example, one may not want to acquire all the individual spectra 'conventionally': for example,

NUS may be used for a HSQC experiment but not for others; or d_1 may be varied for different experiments. These will have an impact on both the durations of the experiments, as well as their sensitivities. To make any meaningful quantitative comparisons, it is therefore necessary to restrict the discussion to values of ρ_t, A, and ε, which can be objectively calculated. This is the approach I have taken in this thesis. These should of course be read with the qualitative understanding that depending on the context, these aforementioned factors may lead to *some*—but never a *complete*—decrease in the utility of NOAH experiments.

4.1.2 Magnetisation pools

subsec:noah__magpools

Having gotten this relatively dry material out of the way, I now turn to exactly how NOAH supersequences are constructed. Ordinarily, if the recovery delay is removed from an NMR experiment, its sensitivity will be greatly reduced because insufficient magnetisation will have recovered between repetitions; or in other words, $A^{(i)}$ will be very small. Such experiments would only really be useful well in the sampling-limited regime.

The key to avoiding this in NOAH supersequences is to make sure that *each module samples a different source of magnetisation*. For example, a HSQC module can be designed to only sample magnetisation of protons directly bonded to the 1.1%-natural abundance ^{13}C, and leave all other proton magnetisation untouched. Immediately following this, the remainder of the proton magnetisation can then be used to record (say) a COSY module, without needing a separate recovery delay. Using the notation of Orts and Gossert,[36] the magnetisation of ^{13}C–bound protons is denoted as $^1\mathrm{H}^{\mathrm{C}}$, and the magnetisation of protons *not* bonded to ^{13}C is denoted as $^1\mathrm{H}^{!\mathrm{C}}$. Protons not directly bonded to NMR-active heteronuclei are labelled $^1\mathrm{H}^{!\mathrm{X}}$, and will often be referred to as 'bulk' magnetisation, since (in natural-abundance samples) the majority of protons fall into this category.

Most standard 2D experiments do not preserve unused magnetisation but instead dephase it through CTP gradient selection; thus, NOAH modules often require some modifications compared to standard experiments. For example, compared to the echo–antiecho HSQC (discussed in § 1.4.5), the NOAH HSQC module[30] adds an extra CTP gradient so that the bulk magnetisation is refocused and ultimately returned to the $+z$ equilibrium state (fig. 4.2). (This is largely identical to the 'symmetrised' ASAP-HSQC experiment.[37])

Sometimes, the modifications required are more extensive, as in the HMBC module. If this module is followed by a HSQC module (or any other module which draws on $^1\mathrm{H}^{\mathrm{C}}$ magnetisation), the initial 90° excitation pulse must be replaced with a zz-filter (fig. 4.3). This performs an *isotope-selective rotation* in that $^1\mathrm{H}^{\mathrm{C}}$ magnetisation is stored along the z-axis, but $^1\mathrm{H}^{!\mathrm{C}}$ magnetisation is excited (and subsequently detected). In general, sequences which are thus modified have lower

fig:noah_hsqc

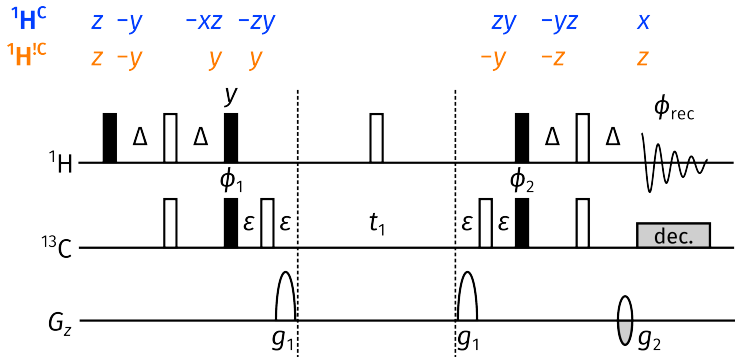

Figure 4.2: NOAH HSQC module. The delay Δ is set to $1/(4 \cdot {}^1J_{\mathrm{CH}})$. Phase cycling is performed with $\phi_1 = (x, -x)$, $\phi_2 = (x, x, -x, -x)$, and $\phi_{\mathrm{rec}} = (x, -x, -x, x)$. Gradient amplitudes are $(g_1, g_2) = (80\%, \pm 40.2\%)$. The notation for product operator analysis is explained in the *Preface*.

sensitivities (i.e. $A < 1$) than the 'original' sequences from which they were derived.

fig:noah_hmbc_no90_po

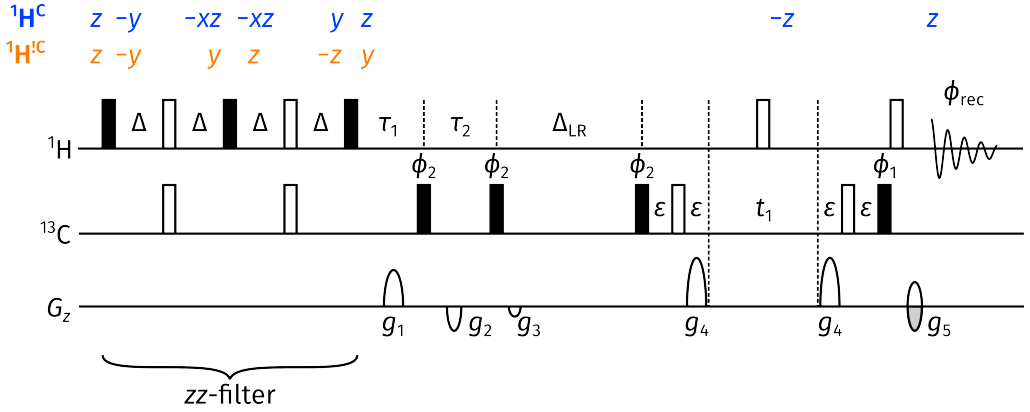

Figure 4.3: NOAH HMBC module. Delays are set as: $\Delta = 1/(2 \cdot {}^nJ_{\mathrm{CH}})$; $\tau_1 = 1/(2 \cdot {}^1J_{\mathrm{CH,max}})$; $\tau_2 = 1/(2 \cdot {}^1J_{\mathrm{CH,min}})$ (see also § 3.4.7). Phase cycling is performed with $\phi_1 = (x, -x)$, $\phi_2 = (x, x, -x, -x)$, and $\phi_{\mathrm{rec}} = (x, -x, -x, x)$. Gradient amplitudes are $(g_1, g_2, g_3, g_4, g_5) = (15\%, -10\%, -5\%, 80\%, \pm 40.2\%)$.

In contrast, modules placed towards the *end* of a supersequence do not need to be modified, as they do not need to preserve any magnetisation. This includes virtually all homonuclear modules, which are allowed to simply consume any remaining magnetisation. Although this makes their implementation very straightforward, in general these modules will *also* suffer some losses in sensitivity, because the preceding modules do not perfectly retain all magnetisation.

Thus, in general, it is not possible for any module in a NOAH supersequence to have $A = 1$,

unless it is placed first in the supersequence *and* has not undergone any modifications.* Such cases are very rare, and it is thus necessary to accept some decreases in A, which are often fairly small (on the order of 10–20%). In the sampling-limited regime, sensitivity is not at a premium and this is often perfectly tolerable. In the sensitivity-limited regime, the full time savings ρ_t cannot be realised, but since ε is still typically larger than 1, there is still an overall boost in sensitivity per unit time.

4.1.3 Case studies

sec:noah__case_studies

Using all that has been described in the previous sections, we now look at a few 'typical' supersequences to understand their construction. A quick note about the nomenclature of NOAH supersequences is warranted here. Supersequences are labelled by the number of modules N, plus a series of single-letter codes corresponding to the identity and ordering of the modules involved (table 4.1). Occasionally, superscripts or subscripts are used to qualify the modules involved.† Thus, a NOAH supersequence containing three modules—say ^{15}N HMQC, ^{13}C HSQC, and CLIP-COSY—would be referred to as a NOAH-3 $\mathrm{M_N SC^c}$. Table 4.2 provides values of ρ_t and A for each module of several typical supersequences, which will be rationalised in the text which follows.

NOAH-2 SC: HSQC + COSY

We begin with perhaps the simplest example of a NOAH supersequence, one containing the HSQC and COSY modules: this is labelled as a NOAH-2 SC experiment (entry 1, table 4.2). As shown in fig. 4.2, the HSQC module only samples $^1\mathrm{H}^{\mathrm{C}}$ magnetisation, and leaves $^1\mathrm{H}^{\mathrm{!C}}$ magnetisation along the $+z$-axis Although the HSQC experiment has to be modified to preserve this $^1\mathrm{H}^{\mathrm{!C}}$ magnetisation, its sensitivity is practically unaffected as compared to a 'standard' HSQC ($A = 0.97$). Furthermore, the COSY module retains *most* of its sensitivity ($A = 0.90$). The small loss here is because the HSQC module does not *perfectly* preserve the $^1\mathrm{H}^{\mathrm{!C}}$ magnetisation: for example, evolution of J-couplings as well as relaxation occur during the HSQC pulse sequence, which are ignored in the product operator analysis in fig. 4.2.

The value of the time-saving factor, $\rho_t = 1.87$, is very close to the theoretical limit of $N = 2$. This reflects the fact that the pulse sequence itself, τ_{ps}, is fairly short for both the HSQC and COSY

*Of course, this also depends on exactly *what* standalone experiment the NOAH supersequence is being compared against. Sometimes, in the literature, the NOAH experiment has been compared against its constituent modules acquired in a standalone fashion; in this case, the first module will always have $A = 1$. This tells us how much we gain through the act of concatenating modules, but is less meaningful in the 'real world' where one is interested in how useful NOAH is relative to 'typical' optimised 2D experiments. I therefore prefer to make comparisons against standard-library sequences.

†With the increasing number of modules, and the variety of modern NMR experiments which could be incorporated into NOAH supersequences, keeping these abbreviations short yet meaningful has been a challenge.

^{1}H–^{15}N modules		^{1}H–^{13}C modules		^{1}H–^{1}H modules	
Module	Code	Module	Code	Module	Code
HMQC	M_N	HSQC	S	COSY	C
HSQC	S_N	seHSQC	S^+	CLIP-COSY	C^c
seHSQC	S_N^+	HSQC-TOCSY	S^T	DQF-COSY	C
HMBC	B_N	HSQC-COSY	S^C	TOCSY	T
		2BOB	O	NOESY	N
		HMBC	B	ROESY	R
		ADEQUATE	A	PSYCHE	P
				TSE-PSYCHE	P^T
				PSYCHE 2DJ	J

tbl:noah_modules

Table 4.1: A (non-exhaustive) list of single-letter module codes for a selection of NOAH modules. Note that, in the literature, the ^{15}N HMQC module has been referred to simply by 'M', since the HSQC module is preferred for ^{1}H–^{13}C correlations. In this thesis, I include the subscript N throughout to avoid any ambiguity.

Entry	Sequence	τ_{NOAH}	ρ_t	A				
				HMBC	seHSQC	HSQC	COSY	TOCSY
1	SC	15 min 0 s	1.87			0.97	0.90	
2	SCT	16 min 25 s	2.60			1.01	0.99	0.79
3	BS	15 min 40 s	1.82	0.93		0.87		
4	SB	15 min 35 s	1.83	0.99		0.96		
5	BSCT	17 min 48 s	3.22	0.95		0.90	0.36	0.28
6	BS_N^+SCT	18 min 57 s	3.74	0.95	0.71	0.66	0.38	0.30
7	S_N^+BSCT	18 min 56 s	3.75	0.76	0.79	0.74	0.33	0.26

tbl:noah_sensitivities

Table 4.2: Sensitivity and time-saving analyses of several typical NOAH supersequences. All experiments were acquired with 2 scans per increment, 256 t_1 increments, an acquisition time of 67 ms, and a recovery delay of 1.5 s. The following Bruker library sequences were used as the 'conventional' experiments: `hmbcetgpl2nd`, `hsqcetf3gpsi2`, `hsqcetgpsp.2`, `cosygpqf`, and `dipsi2gpphzs`. *Data code:* `7Z-220224`.

modules; the deviation therefore chiefly arises from the acquisition time, τ_{acq}. In all respects, this is therefore an example of an 'ideal' NOAH supersequence, where the combination of two modules provides time savings without compromising on sensitivity.

It is worth pointing out that the order of the modules cannot be reversed: the COSY module cannot be (easily) modified to preserve $^1H^C$ magnetisation. In a hypothetical NOAH-2 CS supersequence, the later HSQC module would only be able to use magnetisation recovered during the COSY FID, leading to substantial sensitivity drops.

A final point to consider would be whether the NOAH data has comparable spectral quality in

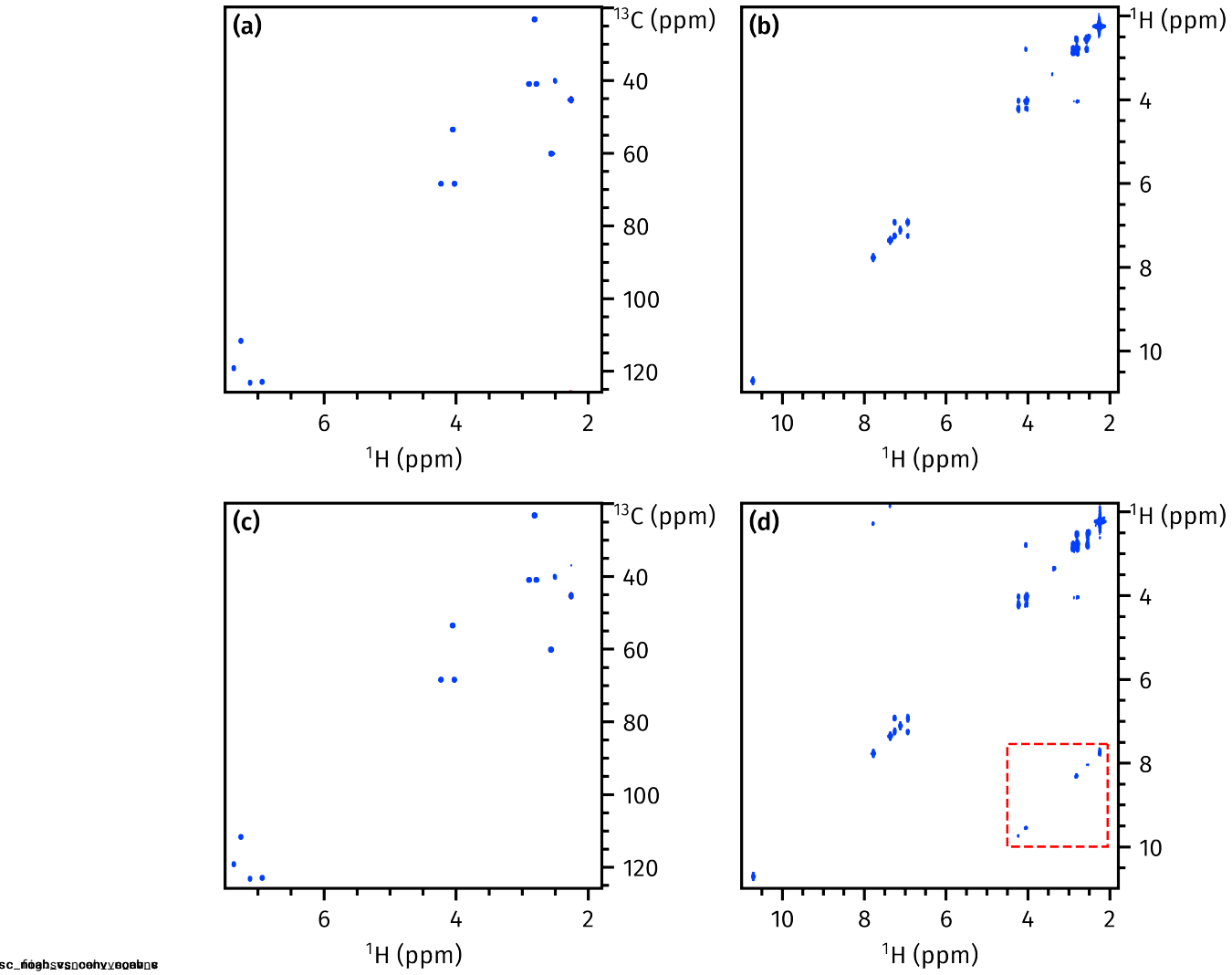

Figure 4.4: **(a)** HSQC from NOAH-2 SC supersequence. **(b)** COSY from NOAH-2 SC supersequence. **(c)** Standalone HSQC. **(d)** Standalone COSY; off-diagonal artefacts are highlighted in the red box. *Data code:* `7Z-220224`.

terms of (for example) artefacts. In this case, the answer is yes: the NOAH HSQC spectrum is virtually identical to the standalone (figs. 4.4a and 4.4c; both spectra have low-level artefacts of different kinds, which do not seriously impede the interpretation and are not shown). On the other hand, the NOAH COSY spectrum seems to actually *improve* on the standalone COSY, in that it better suppresses off-diagonal artefacts (figs. 4.4b and 4.4d). These artefacts likely arise in the standalone COSY because of accidental refocusing of magnetisation which has not completely relaxed between t_1 increments.[38] In contrast, the NOAH COSY module has an extra set of HSQC gradients between every repetition of the COSY, so accidental refocusing is less likely. (Similar artefacts have been noted before in the DQF-COSY experiment,[39,40] and have also shown to be attenuated in the corresponding NOAH module.[41]) That said, such improvements are not always guaranteed: there are sometimes artefacts which arise uniquely in NOAH experiments,

some of which are discussed in the following sections.

NOAH-3 SCT: HSQC + COSY + TOCSY

Evidently, the fact that the HSQC preserves almost all $^1H^{!C}$ magnetisation means that *any* homonuclear module—or a combination thereof—can be placed after it. In general, since homonuclear modules tend to consume any remaining bulk magnetisation, it is very difficult to create combinations of homonuclear modules which do not lead to significant reductions in sensitivity. The only real exceptions are COSY/X combinations, where X can be NOESY, ROESY, or TOCSY: instead of concatenating the COSY and X modules, the COSY pulse sequence can instead be nested *within* the X module, as was first demonstrated with X = NOESY.[42,43] Here, we use the COSY/TOCSY combination as an example.[44] The COSY, TOCSY, and combined COSY/TOCSY modules are shown in fig. 4.5.

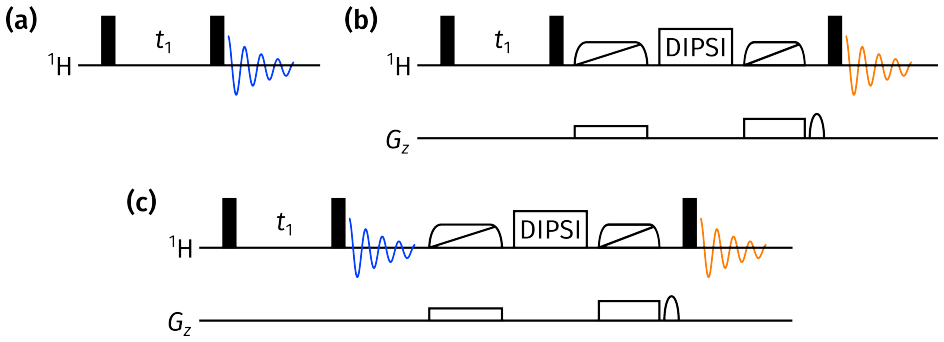

Figure 4.5: **(a)** COSY module. **(b)** TOCSY module; zero-quantum suppression is employed before and after the isotropic mixing period. **(c)** Combined COSY/TOCSY module, where the COSY FID is acquired immediately before the TOCSY mixing.

As shown in table 4.2 (entry 2), this nesting of the COSY module does not materially affect the TOCSY sensitivity. A small loss of approximately 20% is observed, which is partly due to the imperfect magnetisation preservation by the HSQC, and perhaps also due to relaxation during the COSY acquisition period. As for the time-saving factor, a slightly larger deviation ($\rho_t = 2.60$) is observed from the ideal value of 3. This reflects the addition of a TOCSY mixing period, which contributes to τ_{ps}.

NOAH-2 BS: HMBC + HSQC

As mentioned previously, the HMBC module shown in fig. 4.3 is designed to retain $^1H^C$ magnetisation through the addition of the *zz*-filter. This can be used in a subsequent HSQC module in a NOAH-2 BS supersequence. Entry 3 of table 4.2 shows that the addition of the *zz*-filter to eh HMBC causes a relatively small 7% decrease in sensitivity; on the other hand, the HSQC loses 13% of its sensitivity because of incomplete magnetisation preservation.

Generally, it has been recommended that less sensitive modules are placed earlier in the supersequence so that they can access a larger proportion of the equilibrium magnetisation. Since the HMBC is less sensitive of the two modules, this rule of thumb suggests that the BS supersequence would be better than the alternative SB supersequence. In fact, the opposite is true, as entry 4 of table 4.2 shows. The HSQC module has a boost in sensitivity because it is placed first in the supersequence, and no longer needs to rely on the $^{1}H^{C}$ magnetisation preserved by the HMBC; and the HMBC also benefits because the *zz*-filter modification is no longer needed. Arguably, the ordering of modules in a supersequence should be considered on a case-by-case basis.

NOAH-4 BSCT: HMBC + HSQC + COSY + TOCSY

We now move on to a longer supersequence containing four modules, with a correspondingly larger ρ_t value of 3.22. The sensitivity of the HSQC module is practically the same as in the NOAH-2 BS supersequence just described: however, the COSY and TOCSY modules expose one weakness of the HMBC module which has so far been overlooked. In principle, the HMBC module should only excite magnetisation of protons which are long-range coupled to ^{13}C (which we could, for example, denote as $^{1}H^{C(LR)}$). This magnetisation pool should be separate from both the directly coupled protons ($^{1}H^{C}$), as well as protons which are not coupled to any ^{13}C at all ($^{1}H^{!C}$). Unfortunately, this is not the case: it is not actually possible to separate the $^{1}H^{C(LR)}$ and $^{1}H^{!C}$ magnetisation pools. The HMBC excites both of these magnetisation sources, dephases the latter using CTP gradients, and detects the signal arising from the former.

What this means, of course, is that the COSY/TOCSY module which rely on $^{1}H^{!C}$ magnetisation will have substantially lower sensitivities. The signal detected in these two modules derives only from whatever has recovered during the previous two acquisition periods, as shown in entry 5 of table 4.2: A for COSY and TOCSY is 0.36 and 0.28 respectively. That said, this is in fact not likely to be an issue *even* for sensitivity-limited samples. Because the intrinsic sensitivity of the HMBC is orders of magnitude lower than the COSY and TOCSY, even with these large losses in sensitivity, the COSY and TOCSY spectra still have greater intensities than the HMBC. Thus, as long as the entire supersequence is acquired with enough scans to make the HMBC SNR sufficient, the SNR in the COSY and TOCSY will *also* be acceptable. This is illustrated in fig. 4.6.

A rather more insidious problem is that different signals relax at different rates: thus, the COSY and TOCSY spectra (or indeed, any homonuclear module) will have uneven intensities and are frequently asymmetric. This can be seen in the COSY spectrum, where a pair of asymmetric crosspeaks are highlighted. Adding a period of isotropic mixing before the COSY module[45] can help to ameliorate this to some extent (this was not performed when acquiring the data in fig. 4.6).

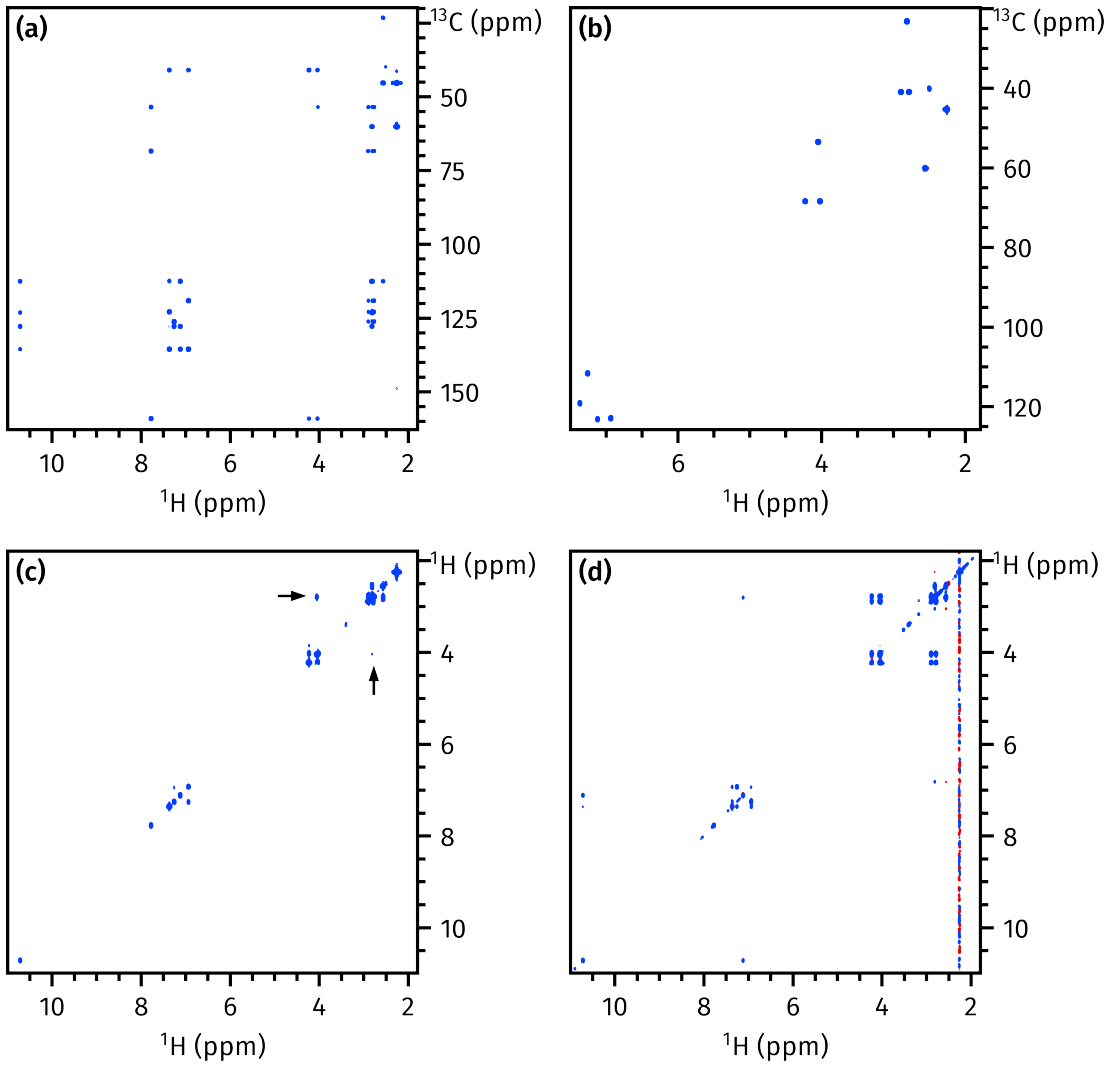

fig_bsbtc

Figure 4.6: Spectra obtained from a NOAH-4 BSCT supersequence. **(a)** HMBC. **(b)** HSQC. **(c)** COSY; a pair of asymmetric crosspeaks are highlighted with red arrows. **(d)** TOCSY (60 ms DIPSI-2 mixing). Despite the COSY and TOCSY having only ~ 30% sensitivity compared to standalone experiments, the intensity of the spectra obtained is still perfectly acceptable (the contour levels chosen are 1–2 orders of magnitude larger than for the HMBC). *Data code:* `7Z-220224`.

NOAH-5 BS$^{+}_{N}$SCT: HMBC + ^{15}N seHSQC + HSQC + COSY + TOCSY

As the final example, we add a further magnetisation pool to the mix, namely protons directly coupled to ^{15}N (i.e. ^{1}H^{N}). As of the time of writing, the implementation of multiple-FID experiments on Bruker spectrometers limits N to a maximum of 5, so a supersequence such as the present NOAH-5 BS$^{+}_{N}$SCT is the current limit. (However, there is no *scientific* argument forbidding $N > 5$, and it is likely that in future versions of TopSpin this restriction will be lifted.)

The values of A for each module are given in entry 6 of table 4.2. If the HMBC module is placed at

the beginning of the supersequence, then in order to preserve *both* $^{1}H^{N}$ and $^{1}H^{C}$ magnetisation, the *zz*-filter must be extended to include ^{15}N pulses.[46] As before, the ^{15}N seHSQC and ^{13}C HSQC modules both suffer drops in sensitivity. For the ^{15}N seHSQC, this is partly because of imperfect preservation of $^{1}H^{N}$ magnetisation by the HMBC, but also stems from the addition of the *zz* isotope-selective pulse (ZIP) element to the seHSQC pulse sequence; this is described further in § 4.3.2. On the other hand, for the ^{13}C HSQC, the sensitivity loss stems purely from imperfect retention of $^{1}H^{C}$ magnetisation. Finally, because the HMBC dephases $^{1}H^{IX}$ magnetisation, the COSY and TOCSY at the end have lower sensitivities: however, as discussed above, this is not an issue in practice.

It is also possible to move the ^{15}N seHSQC module to the front: this gives it a slightly greater sensitivity, at the cost of the HMBC (entry 7, table 4.2). In general, these two modules tend to have comparable sensitivity, and which of these two arrangements is better depends on which module the sensitivity needs to be optimised for.

Lastly, the value of ρ_t given here of 3.74 represents an effective upper limit on the time-saving factor. Although ρ_t increases with N, the extent to which it deviates from the ideal value of N also increases: it is very difficult to obtain $\rho_t > 4$, even with five modules in the supersequence. Of course, it is possible to increase ρ_t further by lengthening the recovery delay d_1 used for the experiments: for example, if d_1 is increased to 2 s from its present value of 1.5 s, ρ_t increases to 3.94. Obviously, this can only be pushed so far before it becomes meaningless.

4.2 GENESIS: automated pulse programme creation

sec:noah__genesis

In this section, I discuss the development of the GENESIS (GENEration of Supersequences In Silico) website (fig. 4.7): as the name suggests, it automatically generates pulse programmes for arbitrary NOAH supersequences. The website also provides extensive instructions on acquiring and processing NOAH data. Although this may at first glance appear slightly out of chronological order, in that the paper[3] was published later than much of the other work in this chapter, an early version of the GENESIS tool was in fact created much earlier (by July 2020).

The present version of GENESIS is available at `https://nmr-genesis.co.uk`; the source code can also be obtained from `https://github.com/yongrenjie/genesis`.

4.2.1 Motivation

ah__genesis_motivation

From the preceding discussion in § 4.1, it is clear that modules which use different magnetisation pools can be combined almost at will. It does not matter *what* modules they are, merely what magnetisation pools they consume (and preserve). Thus, for example, the NOAH-2 SC super-

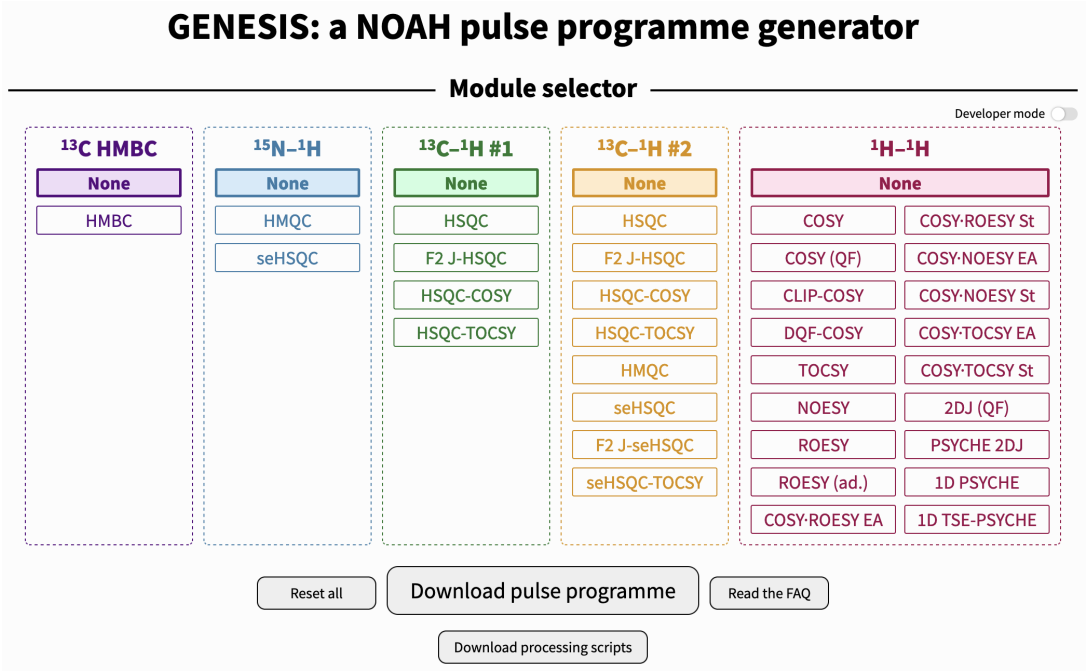

fig:genesis_frontpage

Figure 4.7: The front page of the GENESIS website (https://nmr-genesis.co.uk), as of 10 September 2022.

sequence can in fact be generalised to any $^{1}H^{C}$ module plus any $^{1}H^{!C}$ module. Very broadly speaking, we may define a generic supersequence as having any or all of the following:

- a HMBC module, which actually uses $^{1}H^{!X}$ magnetisation but can be placed at the front as discussed in the NOAH-3 BSC example above;
- a $^{1}H^{N}$ module;
- one or more $^{1}H^{C}$ modules (it is possible to partition the $^{1}H^{C}$ magnetisation pool between two modules, as will be discussed in § 4.3.4);
- one or more $^{1}H^{!X}$ modules which consume bulk magnetisation.

In the first NOAH paper in 2017,[30] a total of 285 'viable' supersequences were already listed. If we further take into account some of the new modules which were developed over the course of my DPhil (§ 4.3), the generic formula above provides for over 4000 viable supersequences.* ('Non-viable' sequences would be those which have undesirable drawbacks: for example, wrongly ordered modules like in a NOAH-2 CS supersequence.)

In spite of this, *only around 45 pulse programmes* had been made available (either via the supplementary information of NOAH papers, or the Bruker User Library). Traditionally, pulse

*This is also ignoring the 'parallel' supersequences, which are discussed in § 4.5. The support for parallel supersequences in GENESIS is not complete: integrating these fully would require substantial changes to the user interface, which I have not had time to do.

programmes must be written by hand, which is a laborious and fairly error-prone process made worse by the sheer length of NOAH experiments. Doing this for thousands of supersequence is clearly impractical; furthermore, each time a new module is developed, or an old module is improved, updating every relevant supersequence would itself already be a mammoth task. This explains why—although the NOAH concept provides a clear blueprint for how supersequences may be constructed—there is still a huge gap between theory and practice.

To bridge this gap, I turned towards the *programmatic* generation of pulse programmes.* This not only allows for existing supersequences to be generated at will, but also provides an easy way for updates to be rapidly disseminated to the NMR community. Furthermore, a website can serve as a 'one-stop' shop where—after downloading pulse programmes—users may download the associated NOAH processing scripts and also access instructions on how to run NOAH experiments. This information did already exist, but was scattered across several different websites and/or journal supplementary information documents, and would have been needlessly confusing to a new user (not to mention the different versions of scripts available in different publications).

4.2.2 Implementation details

genesis_implementation

I will now describe a few features of GENESIS pulse programmes, as well as how these are implemented. The GENESIS code is written in TypeScript; during deployment, this is compiled to JavaScript, which can then be directly executed in the client's web browser. No server-side code is required, meaning that the GENESIS web page is actually a static site (it is currently hosted using GitHub Pages).

Overall structure

The algorithm used for pulse programme construction can loosely be separated into three parts, which are shown in listing 4.1:

1. the *preamble*, which consists of everything up until the beginning of the actual pulse sequence (the `ze` command). This includes header comments as well as definitions of parameters, such as delays and pulse widths;
2. the *main section*, which contains the actual pulse sequence;
3. the *epilogue*, which contains phase cycle information as well as footer comments describing

*This is actually a bit of a lie: GENESIS was initially created for my own convenience. Throughout this chapter, I have had to perform many comparisons of different supersequences, and this tool spared me from having to write everything by hand (and—more often than not—subsequently discover mistakes which invalidated the results). Of course, it soon became apparent that it could find much wider use.

```
/* PREAMBLE */
; gns_noah2-SCqf
; 13C HSQC
; 1H magnitude-mode COSY
"d4          = 0.25s/cnst2"  ; 13C INEPT
"in0         = inf1/2"       ; 13C HSQC increment
"in11        = 2*dw"         ; COSY increment
; ...
define delay DC_HSQCa
"DC_HSQCa    = d4-p14/2"
"l0          = td1/2"        ; TD1/NBL

/* MAIN SECTION */
1 ze
4 d1 st0
  ; MODULE 1 - HSQC
  (p1 ph0):f1
  ; ...
  goscnp ph30 cpd2:f2
  50u do:f2
  2m st
  ; MODULE 2 - COSY
  (p1 ph12):f1
  ; ...
  go=2 ph26
  1m iu1        ; TD1/NBL counter
  1m igrad EA   ; echo-antiecho gradients
  1m id11       ; COSY t1
  30m wr #0 if #0 zd
if "l1 % 2 == 0" {
  1m id0        ; HSQC t1
}
  lo to 4 times l0
exit

/* EPILOGUE */
ph0=0
;gpnam4: SMSQ10.100
;gpz4: 70% (13C CTP)
;cpd2:wvm:wudec: cawurst_d-20(220 ppm, 1.4 ms; L2H)
;d4: 1/4J(CH)
;auprog: noah_hsqc:noah_cosy QF
;module identifiers: C_HSQC H_COSY_QF
;pulse programme created by genesis-v2.2.2, https://nmr-genesis.co.uk
;Sun Sep 11 2022 16:04:54 GMT+0800 (Malaysia Time)
```

Listing 4.1: Abridged GENESIS pulse programme for the NOAH-2 SC supersequence shown in fig. 4.1a.

lst:genesis_sc

each parameter. Instructions for generating shaped pulses using Bruker's WaveMaker software are also included here, as well as instructions for automatic processing (§ 4.2.3), and comments indicating how the pulse programme was generated (for reproducibility purposes).

The construction of the preamble and main section is largely accomplished through the collation of module-specific information, the most important of which are:

- information about the module itself, which go into the header comments;
- parameter definitions, which are collated to form the preamble. Duplicates must be removed here to avoid errors; and
- the pulse programmes themselves, which are directly concatenated to form the main section.

These, as well as other smaller bits of information (e.g. relevant citations, appropriate processing scripts), are stored within `NOAHModule` objects. Each distinct module corresponds to one such object. Therefore, if one wants to add a new module to GENESIS, most of the work can be completed by simply defining a new `NOAHModule` object: no changes to the algorithm itself are needed.

To put the epilogue together, the pulse programme constructed so far is scanned for pulse phases, shaped pulses, and all other parameters. Using predefined lookup tables, GENESIS then outputs pulse phase definitions, WaveMaker directives (where appropriate), and comments containing textual descriptions of each parameter. These comments are mostly cosmetic, but are very useful to the user as they are displayed in the `ased` screen when setting up an experiment. Finally, instructions for automatic processing of the NOAH data (explained in § 4.2.1) are added to the bottom, together with the version number and a timestamp (for reproducibility purposes).

Phase/delay incrementation and looping

Since NOAH experiments are 2D experiments, there is one additional complication: the pulse programme must contain appropriate looping statements, together with pulse phase and delay incrementation, in order to correctly generate the indirect dimension. In many existing NOAH pulse programmes, looping in 2D experiments was written using the equivalent of `for` loops (listing 4.2, *left*). Although this suffices for the vast majority of supersequences, whenever anything must be incremented in a different way (e.g. for parallel supersequences, or the PSYCHE module which uses a different number of t_1 increments), the nested loop structure must be modified. I therefore opted to change the structure to use only one loop, and to control the phase and delay incrementation using modular arithmetic (listing 4.2, *right*). The outcome is entirely equivalent,

but edge cases can be implemented simply by adding another check on the loop counter `L1`.

```
"l0 = td1/4"


1 ze
3 1m
4 d1 st0

  ; ... (pulse sequence goes here)

  ; in inner loop
  1m igrad EA   ; HSQC gradients
  1m id11       ; COSY t1
  30m wr #0 if #0 zd
  lo to 4 times 2

  ; in outer loop
  1m ip5*2      ; HSQC 13C 90
  1m ip30*2     ; HSQC receiver
  1m id0        ; HSQC t1
  lo to 3 times l0



end
```

```
"l0 = td1/2"
"l1 = 0"

1 ze
4 d1 st0


  ; ... (pulse sequence goes here)

  ; on every pass
  1m iu1        ; loop counter
  1m igrad EA   ; HSQC gradients
  1m id11       ; COSY t1
  30m wr #0 if #0 zd

  ; on every second pass
  if "l1 % 2 == 0" {
    1m ip5*2      ; HSQC 13C 90
    1m ip30*2     ; HSQC receiver
    1m id0        ; HSQC t1
  }
  lo to 4 times l0

end
```

Listing 4.2: Implementation of phase/delay incrementation and looping in previous NOAH sequences (*left*, using nested loops) and in GENESIS (*right*, using modular arithmetic).

lst:genesis_looping

Parameter standardisation

Each NOAH module contains a number of parameters, including pulse widths, delays, gradient amplitudes, shaped pulse waveforms. Since different modules are stored separately (as different objects), directly concatenating their pulse programmes may lead to conflicting parameter definitions. GENESIS avoids this by maintaining a global table of parameter definitions which are applied to all modules: when new modules are added, they must be checked against this to ensure that there are no inconsistencies.

In general, where possible, these parameters are chosen to be consistent with pulse programmes in the Bruker standard library: thus, for example, `P1` is the ^{1}H 90° pulse width, and `CNST2` is the $^1J_{CH}$ value used for calculating INEPT delays. This makes it easy to read in parameters either from the *prosol* relation tables in TopSpin, or from other existing parameter sets. Some delays

are module-specific and do not need to be reused, and in standard library sequences, are often labelled as `DELTA1`, `DELTA2`, and so on. To avoid conflicting definitions and also to improve readability, I rename these such that they include the name of the module: thus, in a ^{13}C HSQC these may be labelled `DC_HSQC_1`. Here, `C_HSQC` is the module code, which will be explained further below.

If combined with some caution when adding new modules, these measures ensure that *within* a supersequence there are no parameter clashes: we may view this as a *local uniqueness* of parameters. However, the impact of this design choice is even more far-reaching: since parameters are stored globally, they will always have the same value in *all* possible supersequences (or in other words, the parameters are *globally unique*). This makes it exceptionally easy to set up multiple different supersequences in TopSpin: virtually all of the parameter values may simply be copied from a previous NOAH dataset.

One potential issue with this strategy is that TopSpin provides a finite number of named pulse widths (for example). Thus, there are only so many different parameters which can be stored in a global table before running into inevitable conflicts. A workaround would be to sacrifice the global uniqueness of each parameter, and only have it be unique within a given supersequence. Fortunately, this situation has not (yet) surfaced.*

Parameter descriptions

Module choice

Developer mode

Tests

How smart is GENESIS?

4.2.3 Processing improvements

ah__genesis_processing

4.3 Discussion of individual modules

sec:noah__modules

4.3.1 ^{13}C sensitivity-enhanced HSQC

subsec:noah__sehsqc_c

^{13}C seHSQC

*The number of *pulse phases* in particular, though, is dangerously close to the maximum number of 32. In fact, the global uniqueness criterion is not really important for pulse phases, because—unlike, say, delays—pulse phases are hardcoded in the pulse programme, and cannot be copied from one dataset to another. So, if necessary, I could dispense with the global uniqueness for pulse phases, at the cost of some increased code complexity. I did briefly contemplate this possibility, but since I am at the end of my DPhil and am unlikely to add any new modules soon, this will remain a hypothetical—for now.

4.3.2 ^{15}N sensitivity-enhanced HSQC

subsec:noah__sehsqc_n

^{15}N seHSQC

4.3.3 HMQC

subsec:noah__hmqc

Suppression of wing artefacts (GENESIS paper)

4.3.4 HSQC-TOCSY

subsec:noah__hsqctocsy

HSQC + DIPSI + HSQC combos

Extension to HSQC-TOCSY

Cite ASAP work (Luy)

4.3.5 HSQC-COSY

subsec:noah__hsqccosy

Comparison of several versions of HSQC-COSY (JACS Au SI)

4.3.6 2DJ and PSYCHE

subsec:noah__2djpsyche

cnst37 scaling

SAPPHIRE

4.3.7 HMBC

subsec:noah__hmbc

Suppression of $^{1}J_{CH}$ artefacts (GENESIS paper)

Investigation of gradient schemes (no difference was really observed, but that's fine)

Also ^{15}N HMBC

4.3.8 ADEQUATE

subsec:noah__adequate

Recent stuff.

4.4 Solvent suppression in NOAH

sec:noah__solvsupp

GENESIS paper.

4.5 Parallel and generalised NOAH supersequences

sec:noah__parallel

Blah.

4.6 References

Yong2021JMR (1) Yong, J. R. J.; Hansen, A. L.; Kupče, Ē.; Claridge, T. D. W. Increasing sensitivity and versatility in NMR supersequences with new HSQC-based modules. *J. Magn. Reson.* **2021**, *329*, 107027, DOI: 10.1016/j.jmr.2021.107027.

Kupce2021JACSA (2) Kupče, Ē.; Yong, J. R. J.; Widmalm, G.; Claridge, T. D. W. Parallel NMR Supersequences: Ten Spectra in a Single Measurement. *JACS Au* **2021**, *1*, 1892–1897, DOI: 10.1021/jacsau.1c00423.

Yong2022AC (3) Yong, J. R. J.; Kupče, Ē.; Claridge, T. D. W. Modular Pulse Program Generation for NMR Supersequences. *Anal. Chem.* **2022**, *94*, 2271–2278, DOI: 10.1021/acs.analchem.1c04964.

Yong2022_ABBS (4) Yong, J. R. J.; Kupče, Ē.; Claridge, T. D. W. Uniting Low- and High-Sensitivity Experiments through Generalised NMR Supersequences. **2022**, manuscript in preparation.

Kupce2021NRMP (5) Kupče, Ē.; Frydman, L.; Webb, A. G.; Yong, J. R. J.; Claridge, T. D. W. Parallel nuclear magnetic resonance spectroscopy. *Nat. Rev. Methods Primers* **2021**, *1*, No. 27, DOI: 10.1038/s43586-021-00024-3.

Yong2022RSCBook (6) Yong, J. R. J.; Kupče, Ē.; Claridge, T. D. W. In *Fast 2D solution-state NMR: concepts and applications*, Giraudeau, P., Dumez, J.-N., Eds., forthcoming, 2022.

Barna1987JMR (7) Barna, J. C. J.; Laue, E. D.; Mayger, M. R.; Skilling, J.; Worrall, S. J. P. Exponential sampling, an alternative method for sampling in two-dimensional NMR experiments. *J. Magn. Reson.* **1987**, *73*, 69–77, DOI: 10.1016/0022-2364(87)90225-3.

Kazimierczuk2010PNMRS (8) Kazimierczuk, K.; Stanek, J.; Zawadzka-Kazimierczuk, A.; Koźmiński, W. Random sampling in multidimensional NMR spectroscopy. *Prog. Nucl. Magn. Reson. Spectrosc.* **2010**, *57*, 420–434, DOI: 10.1016/j.pnmrs.2010.07.002.

Mobli2014PNMRS (9) Mobli, M.; Hoch, J. C. Nonuniform sampling and non-Fourier signal processing methods in multidimensional NMR. *Prog. Nucl. Magn. Reson. Spectrosc.* **2014**, *83*, 21–41, DOI: 10.1016/j.pnmrs.2014.09.002.

Kazimierczuk2015MRC (10) Kazimierczuk, K.; Orekhov, V. Non-uniform sampling: post-Fourier era of NMR data collection and processing. *Magn. Reson. Chem.* **2015**, *53*, 921–926, DOI: 10.1002/mrc.4284.

eSunninghausen2014JACS (11) Schulze-Sünninghausen, D.; Becker, J.; Luy, B. Rapid Heteronuclear Single Quantum Correlation NMR Spectra at Natural Abundance. *J. Am. Chem. Soc.* **2014**, *136*, 1242–1245, DOI: 10.1021/ja411588d.

Schanda2006JACS (12) Schanda, P.; Van Melckebeke, H.; Brutscher, B. Speeding Up Three-Dimensional Protein NMR Experiments to a Few Minutes. *J. Am. Chem. Soc.* **2006**, *128*, 9042–9043, DOI: 10.1021/ja062025p.

Kupce2007MRC (13) Kupče, Ē.; Freeman, R. Fast multidimensional NMR by polarization sharing. *Magn. Reson. Chem.* **2007**, *45*, 2–4, DOI: 10.1002/mrc.1931.

Schanda2009PNMRS (14) Schanda, P. Fast-pulsing longitudinal relaxation optimized techniques: Enriching the toolbox of fast biomolecular NMR spectroscopy. *Prog. Nucl. Magn. Reson. Spectrosc.* **2009**, *55*, 238–265, DOI: 10.1016/j.pnmrs.2009.05.002.

Frydman2002PNASUSA (15) Frydman, L.; Scherf, T.; Lupulescu, A. The acquisition of multidimensional NMR spectra within a single scan. *Proc. Natl. Acad. Sci. U. S. A.* **2002**, *99*, 15858–15862, DOI: 10.1073/pnas.252644399.

Pelupessy2003JACS (16) Pelupessy, P. Adiabatic Single Scan Two-Dimensional NMR Spectrocopy. *J. Am. Chem. Soc.* **2003**, *125*, 12345–12350, DOI: 10.1021/ja034958g.

Frydman2003JACS (17) Frydman, L.; Lupulescu, A.; Scherf, T. Principles and Features of Single-Scan Two-Dimensional NMR Spectroscopy. *J. Am. Chem. Soc.* **2003**, *125*, 9204–9217, DOI: 10.1021/ja030055b.

Tal2010PNMRS (18) Tal, A.; Frydman, L. Single-scan multidimensional magnetic resonance. *Prog. Nucl. Magn. Reson. Spectrosc.* **2010**, *57*, 241–292, DOI: 10.1016/j.pnmrs.2010.04.001.

Gouilleux2018ARNMRS (19) Gouilleux, B.; Rouger, L.; Giraudeau, P. Ultrafast 2D NMR: Methods and Applications. *Annu. Rep. NMR Spectrosc.* **2018**, 75–144, DOI: 10.1016/bs.arnmr.2017.08.003.

Kupce2003JMR (20) Kupče, Ē.; Freeman, R. Two-dimensional Hadamard spectroscopy. *J. Magn. Reson.* **2003**, *162*, 300–310, DOI: 10.1016/s1090-7807(02)00196-9.

Kupce2003PNMRS (21) Kupče, E.; Nishida, T.; Freeman, R. Hadamard NMR spectroscopy. *Prog. Nucl. Magn. Reson. Spectrosc.* **2003**, *42*, 95–122, DOI: 10.1016/s0079-6565(03)00022-0.

Jeannerat2000MRC (22) Jeannerat, D. High resolution in the indirectly detected dimension exploiting the processing of folded spectra. *Magn. Reson. Chem.* **2000**, *38*, 415–422, DOI: 10.1002/1097-458x(200006)38:6<415::aid-mrc665>3.0.co;2-u.

Bermel2009JACS (23) Bermel, W.; Bertini, I.; Felli, I. C.; Pierattelli, R. Speeding Up ^{13}C Direct Detection Biomolecular NMR Spectroscopy. *J. Am. Chem. Soc.* **2009**, *131*, 15339–15345, DOI: 10.1021/ja9058525.

Njock2010C (24) Njock, G. B. B.; Pegnyemb, D. E.; Bartholomeusz, T. A.; Christen, P.; Vitorge, B.; Nuzillard, J.-M.; Shivapurkar, R.; Foroozandeh, M.; Jeannerat, D. Spectral Aliasing: A Super Zoom for 2D-NMR Spectra. Principles and Applications. *Chimia* **2010**, *64*, 235, DOI: 10.2533/chimia.2010.235.

Nolis2007ACIE (25) Nolis, P.; Pérez-Trujillo, M.; Parella, T. Multiple FID Acquisition of Complementary HMBC Data. *Angew. Chem. Int. Ed.* **2007**, *46*, 7495–7497, DOI: 10.1002/anie.200702258.

Parella2010CMR (26) Parella, T.; Nolis, P. Time-shared NMR experiments. *Concepts Magn. Reson.* **2010**, *36A*, 1–23, DOI: 10.1002/cmr.a.20150.

Kupce2006JACS (27) Kupče, Ē.; Freeman, R.; John, B. K. Parallel Acquisition of Two-Dimensional NMR Spectra of Several Nuclear Species. *J. Am. Chem. Soc.* **2006**, *128*, 9606–9607, DOI: 10.1021/ja0634876.

Kupce2008JACS (28) Kupče, Ē.; Freeman, R. Molecular Structure from a Single NMR Experiment. *J. Am. Chem. Soc.* **2008**, *130*, 10788–10792, DOI: 10.1021/ja8036492.

Kovacs2016MRC (29) Kovacs, H.; Kupče, Ē. Parallel NMR spectroscopy with simultaneous detection of1H and19F nuclei. *Magn. Reson. Chem.* **2016**, *54*, 544–560, DOI: 10.1002/mrc.4428.

Kupce2017ACIE (30) Kupče, Ē.; Claridge, T. D. W. NOAH: NMR Supersequences for Small Molecule Analysis and Structure Elucidation. *Angew. Chem. Int. Ed.* **2017**, *56*, 11779–11783, DOI: 10.1002/anie.201705506.

Kupce2021PNMRS (31) Kupče, Ē.; Mote, K. R.; Webb, A.; Madhu, P. K.; Claridge, T. D. W. Multiplexing experiments in NMR and multi-nuclear MRI. *Prog. Nucl. Magn. Reson. Spectrosc.* **2021**, *124–125*, 1–56, DOI: 10.1016/j.pnmrs.2021.03.001.

Nagy2019CC (32) Nagy, T. M.; Gyöngyösi, T.; Kövér, K. E.; Sørensen, O. W. BANGO SEA XLOC/HMBC–H2OBC: complete heteronuclear correlation within minutes from one NMR pulse sequence. *Chem. Commun.* **2019**, *55*, 12208–12211, DOI: 10.1039/c9cc06253j.

Nagy2020JMR (33) Nagy, T. M.; Kövér, K. E.; Sørensen, O. W. Double and adiabatic BANGO for concatenating two NMR experiments relying on the same pool of magnetization. *J. Magn. Reson.* **2020**, *316*, 106767, DOI: 10.1016/j.jmr.2020.106767.

Nagy2021ACIE (34) Nagy, T. M.; Kövér, K. E.; Sørensen, O. W. NORD: NO Relaxation Delay NMR Spectroscopy. *Angew. Chem. Int. Ed.* **2021**, *60*, 13587–13590, DOI: 10.1002/anie.202102487.

Timari2022CC (35) Timári, I.; Nagy, T. M.; Kövér, K. E.; Sørensen, O. W. Synergy and sensitivity-balance in concatenating experiments in NO relaxation delay NMR (NORD). *Chem. Commun.* **2022**, *58*, 2516–2519, DOI: 10.1039/d1cc06663c.

Orts2018M (36) Orts, J.; Gossert, A. D. Structure determination of protein-ligand complexes by NMR in solution. *Methods* **2018**, *138-139*, 3–25, DOI: 10.1016/j.ymeth.2018.01.019.

zeSunninghausen2017JMR (37) Schulze-Sünninghausen, D.; Becker, J.; Koos, M. R. M.; Luy, B. Improvements, extensions, and practical aspects of rapid ASAP-HSQC and ALSOFAST-HSQC pulse sequences for studying small molecules at natural abundance. *J. Magn. Reson.* **2017**, *281*, 151–161, DOI: 10.1016/j.jmr.2017.05.012.

Vitorge2010JMR (38) Vitorge, B.; Bodenhausen, G.; Pelupessy, P. Speeding up nuclear magnetic resonance spectroscopy by the use of SMAll Recovery Times – SMART NMR. *J. Magn. Reson.* **2010**, *207*, 149–152, DOI: 10.1016/j.jmr.2010.07.017.

Shaw1996JMRSA (39) Shaw, A. A.; Salaun, C.; Dauphin, J.-F.; Ancian, B. Artifact-Free PFG-Enhanced Double-Quantum-Filtered COSY Experiments. *J. Magn. Reson., Ser. A* **1996**, *120*, 110–115, DOI: 10.1006/jmra.1996.0105.

Howe2014MRC (40) Howe, P. W. A. Rapid pulsing artefacts in pulsed-field gradient double-quantum filtered COSY spectra. *Magn. Reson. Chem.* **2014**, *52*, 329–332, DOI: 10.1002/mrc.4060.

Claridge2019MRC (41) Claridge, T. D. W.; Mayzel, M.; Kupče, Ē. Triplet NOAH supersequences optimised for small molecule structure characterisation. *Magn. Reson. Chem.* **2019**, *57*, 946–952, DOI: 10.1002/mrc.4887.

Haasnoot1984JMR (42) Haasnoot, C. A. G.; van de Ven, F. J. M.; Hilbers, C. W. COCONOSY. Combination of 2D correlated and 2D nuclear overhauser enhancement spectroscopy in a single experiment. *J. Magn. Reson.* **1984**, *56*, 343–349, DOI: 10.1016/0022-2364(84)90114-8.

Gurevich1984JMR (43) Gurevich, A. Z.; Barsukov, I. L.; Arseniev, A. S.; Bystrov, V. F. Combined COSY-NOESY experiment. *J. Magn. Reson.* **1984**, *56*, 471–478, DOI: 10.1016/0022-2364(84)90311-1.

Nolis2019MRC (44) Nolis, P.; Parella, T. Practical aspects of the simultaneous collection of COSY and TOCSY spectra. *Magn. Reson. Chem.* **2019**, *57*, S85–S94, DOI: 10.1002/mrc.4835.

Kupce2018CC (45) Kupče, Ē.; Claridge, T. D. W. Molecular structure from a single NMR supersequence. *Chem. Commun.* **2018**, *54*, 7139–7142, DOI: 10.1039/c8cc03296c.

Kupce2019JMR (46) Kupče, Ē.; Claridge, T. D. W. New NOAH modules for structure elucidation at natural isotopic abundance. *J. Magn. Reson.* **2019**, *307*, 106568, DOI: 10.1016/j.jmr.2019.106568.

refsection:5